

## ELASTIC WAVE PROPAGATION IN MEDIA WITH PARALLEL FRACTURES AND ALIGNED CRACKS<sup>1</sup>

M. SCHOENBERG<sup>2</sup> and J. DOUMA<sup>3</sup>

### ABSTRACT

SCHOENBERG, M. and DOUMA, J. 1988. Elastic wave propagation in media with parallel fractures and aligned cracks. *Geophysical Prospecting* **36**, 571–590.

A model of parallel slip interfaces simulates the behaviour of a fracture system composed of large, closely spaced, aligned joints. The model admits any fracture system anisotropy: triclinic (the most general), monoclinic, orthorhombic or transversely isotropic, and this is specified by the form of the  $3 \times 3$  fracture system compliance matrix. The fracture system may be embedded in an anisotropic elastic background with no restrictions on the type of anisotropy. To compute the long wavelength equivalent moduli of the fractured medium requires at most the inversion of two  $3 \times 3$  matrices. When the fractures are assumed on average to have rotational symmetry (transversely isotropic fracture system behaviour) and the background is assumed isotropic, the resulting equivalent medium is transversely isotropic and the effect of the additional compliance of the fracture system may be specified by two parameters (in addition to the two isotropic parameters of the isotropic background). Dilute systems of flat aligned microcracks in an isotropic background yield an equivalent medium of the same form as that of the isotropic medium with large joints, i.e. there are two additional parameters due to the presence of the microcracks which play roles in the stress-strain relations of the equivalent medium identical to those played by the parameters due to the presence of large joints. Thus, knowledge of the total of four parameters describing the anisotropy of such a fractured medium tells nothing of the size or concentration of the aligned fractures but does contain information as to the overall excess compliance due to the fracture system and its orientation. As the aligned microcracks, which were assumed to be ellipsoidal, with very small aspect ratio are allowed to become non-flat, i.e. have a growing aspect ratio, the moduli of the equivalent medium begin to diverge from the standard form of the moduli for flat cracks. The divergence is faster for higher crack densities but only becomes significant for microcracks of aspect ratios approaching 0.3.

<sup>1</sup> Presented in part at the 49th EAEG meeting, Belgrade, June 1987; revision accepted February 1988.

<sup>2</sup> Schlumberger-Doll Research, Ridgefield, CT 06877-4108, USA.

<sup>3</sup> Institute for Earth Sciences, Department of Geophysics, PB 80021, 3508 TA Utrecht, The Netherlands.

## INTRODUCTION

It is now clear that there are many regions of the subsurface (some say everywhere) showing azimuthal velocity anisotropy and this has been attributed to the presence of aligned vertical microcracks that arise because of tectonic stresses (see e.g. Crampin 1985; Crampin and Atkinson 1985; Willis, Rethford and Bielanski 1986; Crampin and Bush 1986). That this Crampin model is the actual mechanism causing the azimuthal velocity anisotropy is difficult to say as drilling and coring in such a region distort the stress field locally and perhaps distort and close the cracks that existed in the undeformed rock. A set of robust parameters is needed to give (1) the orientation of the cracks and/or fractures in the subsurface, and (2) a measure of crack density times strength which could be called excess compliance due to the presence of cracks. Such a parameter set could be a valuable indicator of overall stress orientation, and the orientation and strength of the anisotropic part of the permeability tensor. Crack orientation, when cracks are vertical, can be simply determined by the splitting of vertically propagating shear waves. This occurs because of the azimuthal anisotropy induced by microcracks and fractures. The polarization of the faster propagating shear wave according to current theory is parallel to the fractures; the polarization of the slower propagating shear wave is perpendicular to the fractures.

We compare theories that predict elastic anisotropy due to the presence of filled or empty ellipsoidal inclusions with one another and with a theory that predicts elastic anisotropy due to long (compared to wavelength) parallel joints or fractures. For inclusions with small aspect ratios (almost flat cracks), all the models agree with one another and in fact they are indistinguishable from the fracture model. The fracture model is exactly derivable as the limiting case of wave propagation through a region composed of alternating elastic layers. The results for anisotropic layers are reviewed in Section I and the derivation of the fracture model in its most general form and for special cases is presented in detail in Section II. In Section III, the simplest anisotropy attributable to 'transversely isotropic' fractures in an isotropic background is compared in detail with the anisotropy due to systems of aligned flat microcracks. In both the anisotropy is characterized by two, positive, dimensionless parameters that play the same roles in the stress-strain relations. The first depends on the tangential compliance of the joints or cracks and the second depends on the normal compliance. From a phenomenological point of view the behaviour of such systems of aligned flat cracks or parallel joints can be reduced to two numbers which, with the isotropic background moduli, determine the five elastic moduli of a transversely isotropic elastic medium. From the elastic moduli themselves nothing more specific concerning crack density, individual crack compliance or crack size can be found.

However, in Section IV it will be shown that for the ellipsoidal inclusions, as the aspect ratio becomes large (up to 1.0), the moduli derivable from the theory of ellipsoidal inclusions (Nishizawa 1982) deviate from those obtainable from the flat crack or joint theories. This occurs at aspect ratios of about 0.3 for gas- or liquid-filled inclusions at the highest values of crack density of such inclusions for which the theory is thought to be valid.

## I. ELASTIC MODULI OF STRATIFIED MEDIA

Consider a stratified medium made up of perfectly bonded homogeneous, but not necessarily isotropic, layers. Let the  $x_3$ -axis be perpendicular to the layering and assume that there are  $n$  different constituent layers, arranged so that in each sufficiently large interval one finds the same proportion of each medium. The simplest arrangement that satisfies this requirement is a periodic sequence of layers. Each anisotropic constituent has a relative thickness  $h_i$   $i = 1, \dots, n$  so that  $h_1 + \dots + h_n = 1$ , a density  $\rho_i$ , and an elastic modulus tensor  $c_{pqrsi}$ , relating stress  $\sigma_{pq_i}$  with strain  $\epsilon_{rs_i}$ . In condensed notation, for which subscripts  $11 \rightarrow 1$ ,  $22 \rightarrow 2$ ,  $33 \rightarrow 3$ ,  $23 \rightarrow 4$ ,  $31 \rightarrow 5$  and  $12 \rightarrow 6$ , the stress-strain relation may be written

$$\begin{bmatrix} \sigma_1 \\ \sigma_2 \\ \sigma_3 \\ \sigma_4 \\ \sigma_5 \\ \sigma_6 \end{bmatrix} = \begin{bmatrix} c_{11} & c_{12} & c_{13} & c_{14} & c_{15} & c_{16} \\ c_{12} & c_{22} & c_{23} & c_{24} & c_{25} & c_{26} \\ c_{13} & c_{23} & c_{33} & c_{34} & c_{35} & c_{36} \\ c_{14} & c_{24} & c_{34} & c_{44} & c_{45} & c_{46} \\ c_{15} & c_{25} & c_{35} & c_{45} & c_{55} & c_{56} \\ c_{16} & c_{26} & c_{36} & c_{46} & c_{56} & c_{66} \end{bmatrix} \begin{bmatrix} \epsilon_1 \\ \epsilon_2 \\ \epsilon_3 \\ \epsilon_4 \\ \epsilon_5 \\ \epsilon_6 \end{bmatrix} \quad (1)$$

where

$$\begin{bmatrix} \sigma_1 \\ \sigma_2 \\ \sigma_3 \\ \sigma_4 \\ \sigma_5 \\ \sigma_6 \end{bmatrix} = \begin{bmatrix} \sigma_{11} \\ \sigma_{22} \\ \sigma_{33} \\ \sigma_{23} \\ \sigma_{31} \\ \sigma_{12} \end{bmatrix} \quad \text{and} \quad \begin{bmatrix} \epsilon_1 \\ \epsilon_2 \\ \epsilon_3 \\ \epsilon_4 \\ \epsilon_5 \\ \epsilon_6 \end{bmatrix} = \begin{bmatrix} \epsilon_{11} \\ \epsilon_{22} \\ \epsilon_{33} \\ 2\epsilon_{23} \\ 2\epsilon_{31} \\ 2\epsilon_{12} \end{bmatrix}.$$

The elastic moduli for the homogeneous, anisotropic medium equivalent, in the long wavelength (or quasistatic) limit, to a layered medium composed of anisotropic constituent layers, can be expressed in terms of thickness-weighted averages of functions of the moduli of the constituents. The long wavelength assumption on stress is that all stress components acting on surfaces parallel to the layering are the same in all layers, i.e.  $\sigma_{33_i} \equiv \sigma_{3_i} = \sigma_3$ ,  $\sigma_{23_i} \equiv \sigma_{4_i} = \sigma_4$  and  $\sigma_{13_i} \equiv \sigma_{5_i} = \sigma_5$ . The long wavelength kinematic assumption is that over many layers, the layers move together (so that derivatives of in-plane displacements with respect to in-plane coordinates,  $x_1$  and  $x_2$ , are the same) implying that all strain components lying in the plane of the layering are the same in all layers, i.e.  $\epsilon_{11_i} \equiv \epsilon_{1_i} = \epsilon_1$ ,  $\epsilon_{22_i} \equiv \epsilon_{2_i} = \epsilon_2$  and  $2\epsilon_{12_i} \equiv \epsilon_{6_i} = \epsilon_6$ . The other stress and strain components,  $\sigma_{11_i} \equiv \sigma_{1_i}$ ,  $\sigma_{22_i} \equiv \sigma_{2_i}$ ,  $\sigma_{12_i} \equiv \sigma_{6_i}$ ,  $\epsilon_{33_i} \equiv \epsilon_{3_i}$ ,  $2\epsilon_{23_i} \equiv \epsilon_{4_i}$  and  $2\epsilon_{13_i} \equiv \epsilon_{5_i}$ , may vary from layer to layer. In each layer, such a component may be taken as its average value across the thickness of that layer.

A concise way to pose the problem of finding the effective moduli, even when the constituent layers are anisotropic, is through a matrix formulation which distinguishes components that are constant over many layers from the other components which can vary from layer to layer. Following the procedure first outlined

by Helbig and Schoenberg (1987) for general anisotropic layers, define the following vectors

$$\mathbf{S}_{1i} = \begin{bmatrix} \sigma_{1i} \\ \sigma_{2i} \\ \sigma_{6i} \end{bmatrix}, \quad \mathbf{E}_{2i} = \begin{bmatrix} \varepsilon_{3i} \\ \varepsilon_{4i} \\ \varepsilon_{5i} \end{bmatrix}, \quad \text{layer dependent}$$

and

$$\mathbf{S}_2 = \begin{bmatrix} \sigma_3 \\ \sigma_4 \\ \sigma_5 \end{bmatrix}, \quad \mathbf{E}_1 = \begin{bmatrix} \varepsilon_1 \\ \varepsilon_2 \\ \varepsilon_6 \end{bmatrix}, \quad \text{layer independent} \quad (2)$$

which allow the stress-strain relations in any layer to be rewritten as

$$\mathbf{S}_{1i} = \mathbf{M}_i \mathbf{E}_1 + \mathbf{P}_i \mathbf{E}_{2i}, \quad (3a)$$

$$\mathbf{S}_2 = \mathbf{P}_i^T \mathbf{E}_1 + \mathbf{N}_i \mathbf{E}_{2i}. \quad (3b)$$

Here

$$\mathbf{M}_i = \begin{bmatrix} c_{11i} & c_{12i} & c_{16i} \\ c_{12i} & c_{22i} & c_{26i} \\ c_{16i} & c_{26i} & c_{66i} \end{bmatrix}, \quad \mathbf{N}_i = \begin{bmatrix} c_{33i} & c_{34i} & c_{35i} \\ c_{34i} & c_{44i} & c_{45i} \\ c_{35i} & c_{45i} & c_{55i} \end{bmatrix}, \quad \mathbf{P}_i = \begin{bmatrix} c_{13i} & c_{14i} & c_{15i} \\ c_{23i} & c_{24i} & c_{25i} \\ c_{36i} & c_{46i} & c_{56i} \end{bmatrix}, \quad (4)$$

with superscript  $T$  denoting the matrix transpose.  $\mathbf{M}_i$  and  $\mathbf{N}_i$  are symmetrical matrices. Then premultiplying (3b) by  $\mathbf{N}_i^{-1}$  gives

$$\mathbf{N}_i^{-1} \mathbf{S}_2 = \mathbf{N}_i^{-1} \mathbf{P}_i^T \mathbf{E}_1 + \mathbf{E}_{2i}, \quad (5)$$

and solving this for  $\mathbf{E}_{2i}$  and substituting into (3a) yields

$$\mathbf{S}_{1i} = \mathbf{M}_i \mathbf{E}_1 + \mathbf{P}_i (\mathbf{N}_i^{-1} \mathbf{S}_2 - \mathbf{N}_i^{-1} \mathbf{P}_i^T \mathbf{E}_1). \quad (6)$$

Now let the thickness-weighted average over all the constituent layers,  $\sum_{i=1}^n h_i(\cdot)$ , be denoted as  $\langle \cdot \rangle$ . Then taking first, the thickness-weighted average of (6), and second, the thickness-weighted average of (5) and premultiplying this second result by  $\langle \mathbf{N}^{-1} \rangle^{-1}$  gives

$$\langle \mathbf{S}_1 \rangle = [\langle \mathbf{M} \rangle - \langle \mathbf{P} \mathbf{N}^{-1} \mathbf{P}^T \rangle] \mathbf{E}_1 + \langle \mathbf{P} \mathbf{N}^{-1} \rangle \mathbf{S}_2, \quad (7a)$$

$$\mathbf{S}_2 = \langle \mathbf{N}^{-1} \rangle^{-1} \langle \mathbf{N}^{-1} \mathbf{P}^T \rangle \mathbf{E}_1 + \langle \mathbf{N}^{-1} \rangle^{-1} \langle \mathbf{E}_2 \rangle. \quad (7b)$$

Finally substituting the expression for  $\mathbf{S}_2$  from (7b) into (7a) allows us to write the elastic moduli for the media equivalent to the stratified medium in the long wavelength limit, in matrix form as

$$\langle \mathbf{S}_1 \rangle = \mathbf{M}_e \mathbf{E}_1 + \mathbf{P}_e \langle \mathbf{E}_2 \rangle, \quad (8a)$$

$$\mathbf{S}_2 = \mathbf{P}_e^T \mathbf{E}_1 + \mathbf{N}_e \langle \mathbf{E}_2 \rangle, \quad (8b)$$

with

$$\mathbf{N}_e = \langle \mathbf{N}^{-1} \rangle^{-1}, \quad \mathbf{P}_e = \langle \mathbf{P} \mathbf{N}^{-1} \rangle \mathbf{N}_e,$$

$$\mathbf{M}_e = \langle \mathbf{M} \rangle - \langle \mathbf{P} \mathbf{N}^{-1} \mathbf{P}^T \rangle + \langle \mathbf{P} \mathbf{N}^{-1} \rangle \mathbf{N}_e \langle \mathbf{N}^{-1} \mathbf{P}^T \rangle. \quad (9)$$

If the  $i$ th constituent is transversely isotropic with the  $x_3$ -axis, the axis of symmetry, then, from the expressions for  $\mathbf{M}_i$ ,  $\mathbf{N}_i$  and  $\mathbf{P}_i$  in (4), we have

$$\mathbf{M}_i = \begin{bmatrix} c_{11i} & c_{11i} - 2c_{66i} & 0 \\ c_{11i} - 2c_{66i} & c_{11i} & 0 \\ 0 & 0 & c_{66i} \end{bmatrix},$$

$$\mathbf{N}_i = \begin{bmatrix} c_{33i} & 0 & 0 \\ 0 & c_{44i} & 0 \\ 0 & 0 & c_{44i} \end{bmatrix}, \quad \mathbf{P}_i = \begin{bmatrix} c_{13i} & 0 & 0 \\ c_{13i} & 0 & 0 \\ 0 & 0 & 0 \end{bmatrix}. \quad (10)$$

Note that when the  $i$ th constituent layer is isotropic,  $c_{44i} = c_{66i} = \mu_i$ ,  $c_{11i} = c_{33i} = \lambda_i + 2\mu_i$  and  $c_{13i} = \lambda_i$  where  $\lambda_i$  and  $\mu_i$  are Lamé parameters. If all the constituent layers are transversely isotropic, the equivalent homogeneous medium is transversely isotropic and from (9) the moduli are given by

$$\mathbf{N}_e = \begin{bmatrix} c_{33} & 0 & 0 \\ 0 & c_{44} & 0 \\ 0 & 0 & c_{44} \end{bmatrix} = \begin{bmatrix} 1/\langle 1/c_{33} \rangle & 0 & 0 \\ 0 & 1/\langle 1/c_{44} \rangle & 0 \\ 0 & 0 & 1/\langle 1/c_{44} \rangle \end{bmatrix},$$

$$\mathbf{P}_e = \begin{bmatrix} c_{13} & 0 & 0 \\ c_{13} & 0 & 0 \\ 0 & 0 & 0 \end{bmatrix} = \begin{bmatrix} \langle c_{13}/c_{33} \rangle / \langle 1/c_{33} \rangle & 0 & 0 \\ \langle c_{13}/c_{33} \rangle / \langle 1/c_{33} \rangle & 0 & 0 \\ 0 & 0 & 0 \end{bmatrix}, \quad (11)$$

$$\mathbf{M}_e = \begin{bmatrix} c_{11} & c_{11} - 2c_{66} & 0 \\ c_{11} - 2c_{66} & c_{11} & 0 \\ 0 & 0 & c_{66} \end{bmatrix} = \begin{bmatrix} c_{11} & c_{11} - 2\langle c_{66} \rangle & 0 \\ c_{11} - 2\langle c_{66} \rangle & c_{11} & 0 \\ 0 & 0 & \langle c_{66} \rangle \end{bmatrix},$$

$$c_{11} = \langle c_{11} \rangle - \langle c_{13}^2/c_{33} \rangle + \langle c_{13}/c_{33} \rangle^2 / \langle 1/c_{33} \rangle,$$

identical to the results of Backus (1962).

Note that the combination rules (9) are commutative in layer order. If, instead of considering the relative thickness  $h_i$  of each constituent, the combination operation is thought of as the folding together of a total thickness  $H_i$  of each constituent, albeit divided into fine layers, then the combination rules (9) are also associative (Schoenberg and Muir 1988). Thus, if there are three constituents of total thickness  $H_1$ ,  $H_2$  and  $H_3$ , the properties of the combined medium of thickness  $H_1 + H_2 + H_3$  can be determined by first finding the properties of the medium equivalent to constituent 3 mixed with constituent 1, and then stirring in amount  $H_2$  of constituent 2. The resulting equivalent medium is independent of the order of combination.

## II. GENERAL MODEL FOR LONG THIN PARALLEL FRACTURES

The behaviour of long parallel fractures or joints in an otherwise homogeneous anisotropic background medium may be modelled as a set of thin constituent layers, not necessarily isotropic, embedded in the background. The above derived formal-

ism is used and the fractures are modelled by taking the limit as the thickness and the elastic moduli of the embedded thin layers go to zero together. The formalism enables us to identify the effect of even the most anisotropic fractures on the most anisotropic background, and to see the variation in anisotropic behaviour permitted by sets of large parallel fractures. The fracture behaviour is at its simplest if the material inside the fracture is assumed to be transversely isotropic; the assumption of full isotropy implies no further simplification. This type of fracture behaviour is discussed and compared with the behaviour of dilute concentrations of aligned inclusions that may be assumed to model a medium with internal cracks where the cracks have a preferred orientation.

For now, the material inside the fracture is allowed to have arbitrary anisotropy. The fracture-filling material is assumed to be soft by letting the moduli of the fracture layer,  $c_{jk_f}$  be much smaller than a typical non-zero background modulus, say  $c_{33_b}$  (the effect of a hard fracture-filling material would tend to vanish as the fracture widths approached zero). In particular, the moduli are assumed to be of the order of the volume ratio of the fractures  $h_f$ , i.e.  $c_{jk_f}/c_{33_b} = O(h_f)$ . Here  $h_f$  may be thought of as the total fracture thickness in an interval of width  $H$  divided by  $H$ . The interval width  $H$  must satisfy two criteria. It must be sufficiently large so that the fractured medium has the same total thickness of fractures  $h_f H$  in any interval of thickness  $H$ . Yet  $H$  must be much smaller than the smallest wavelength of interest for the fractured medium to be replaced by a long wavelength equivalent homogeneous medium. The assumption on the  $c_{jk_f}$  means that, in the limit, as  $h_f \rightarrow 0$  the  $c_{jk_f}$  may be replaced by  $h_f \tilde{c}_{jk}$  and, from (9) as  $h_f \rightarrow 0$ ,

$$\begin{aligned} \mathbf{N}_e &= \langle \mathbf{N}^{-1} \rangle^{-1} = [(1 - h_f)\mathbf{N}_b^{-1} + h_f \mathbf{N}_f^{-1}]^{-1} \rightarrow (\mathbf{N}_b^{-1} + \tilde{\mathbf{N}}^{-1})^{-1} \\ &= \mathbf{N}_b(\mathbf{I} + \tilde{\mathbf{N}}^{-1}\mathbf{N}_b)^{-1} \end{aligned} \quad (12)$$

$$\mathbf{P}_e \rightarrow (\mathbf{P}_b \mathbf{N}_b^{-1})\mathbf{N}_e, \quad \mathbf{M}_e \rightarrow \mathbf{M}_b - \mathbf{P}_b \mathbf{N}_b^{-1} \mathbf{P}_b^T + (\mathbf{P}_b \mathbf{N}_b^{-1})\mathbf{N}_e(\mathbf{N}_b^{-1} \mathbf{P}_b^T), \quad \langle \rho \rangle \rightarrow \rho_b,$$

where  $\mathbf{I}$  is the  $3 \times 3$  identity matrix. The fracture parameters enter only through  $\tilde{\mathbf{N}}$ , a symmetrical  $3 \times 3$  submatrix of the full  $6 \times 6$  modulus matrix, so that in general there are at most six fracture parameters, the six independent components of  $\tilde{\mathbf{N}}$ . To see why this must be so, consider (3b) for the fracture medium, which gives the components of the stress traction across the fracture. They are

$$\mathbf{S}_2 = h_f \left( \tilde{\mathbf{P}}^T \begin{bmatrix} \varepsilon_1 \\ \varepsilon_2 \\ \varepsilon_6 \end{bmatrix} + \tilde{\mathbf{N}} \begin{bmatrix} \varepsilon_{3_f} \\ \varepsilon_{4_f} \\ \varepsilon_{5_f} \end{bmatrix} \right). \quad (13)$$

Since the fractures are soft, strain components in the fracture layers are large and can be approximated by  $\varepsilon_{3_f} \sim \Delta u_3/h_f H$ ,  $\varepsilon_{4_f} \sim \Delta u_2/h_f H$  and  $\varepsilon_{5_f} \sim \Delta u_1/h_f H$  where  $h_f H$  is the total fracture width in an interval of width  $H$  and  $\Delta u_i$  are the components of the total slip displacement across all the fractures in that interval of width  $H$ . The other strain components in the fracture layers are constrained by the long wavelength assumption to be the same as the corresponding components in the

background medium and thus are not large. Then, in the limit as  $h_f \rightarrow 0$ ,

$$\mathbf{S}_2 = \begin{bmatrix} \sigma_3 \\ \sigma_4 \\ \sigma_5 \end{bmatrix} = \begin{bmatrix} \sigma_{33} \\ \sigma_{23} \\ \sigma_{13} \end{bmatrix} = h_f \left( \tilde{\mathbf{P}}_f^T \begin{bmatrix} \varepsilon_1 \\ \varepsilon_2 \\ \varepsilon_6 \end{bmatrix} + \tilde{\mathbf{N}} \begin{bmatrix} \Delta u_3/h_f H \\ \Delta u_2/h_f H \\ \Delta u_1/h_f H \end{bmatrix} \right) \rightarrow \tilde{\mathbf{N}} \begin{bmatrix} \Delta u_3/H \\ \Delta u_2/H \\ \Delta u_1/H \end{bmatrix}. \quad (14)$$

In subsequent development the 'fracture system compliance matrix'  $\mathbf{Z} \equiv \tilde{\mathbf{N}}^{-1}$  will be used instead of  $\tilde{\mathbf{N}}$  as small slip or vanishing of some components of the fracture system slip-strain will cause  $\tilde{\mathbf{N}}$  to be very large or undefined, while causing  $\mathbf{Z}$  merely to have some small or zero components. Thus (14) becomes

$$\begin{bmatrix} \Delta u_3/H \\ \Delta u_2/H \\ \Delta u_1/H \end{bmatrix} = \mathbf{Z} \begin{bmatrix} \sigma_3 \\ \sigma_4 \\ \sigma_5 \end{bmatrix}. \quad (15)$$

Define the vector on the left, the slip-displacement vector of the fractures in width  $H$  divided by  $H$ , as the 'fracture system slip-strain.' Then  $\mathbf{Z}$  gives the fracture system slip-strain as a linear function of the traction on any  $x_3 = \text{constant}$  surface (Schoenberg, 1980). Note that it is perfectly acceptable that some of the components of  $\mathbf{N}_f \rightarrow 0$  as  $h_f \rightarrow 0$  and for others to remain finite. This is accounted for in the evaluation of the term  $h_f \mathbf{N}_f^{-1}$ , which approaches  $\mathbf{Z}$ , occurring in the first equation of (12) for  $\mathbf{N}_e$ .

Rewriting the first equation of (12) as

$$\mathbf{N}_e = \mathbf{N}_b(\mathbf{I} + \mathbf{Z}\mathbf{N}_b)^{-1}, \quad (16)$$

enables us to write the matrices of the changes from the background moduli due to the fractures, from (12), as

$$\begin{aligned} \Delta \mathbf{N} &= \mathbf{N}_b[(\mathbf{I} + \mathbf{Z}\mathbf{N}_b)^{-1} - \mathbf{I}], \\ \Delta \mathbf{P} &= (\mathbf{P}_b \mathbf{N}_b^{-1})\Delta \mathbf{N}, \quad \Delta \mathbf{M} = (\mathbf{P}_b \mathbf{N}_b^{-1})\Delta \mathbf{N}(\mathbf{N}_b^{-1} \mathbf{P}_b^T). \end{aligned} \quad (17)$$

When  $\mathbf{Z}$  is so small that all terms of  $\mathbf{Z}\mathbf{N}_b \ll 1$ , we see that  $\mathbf{N}_e \approx \mathbf{N}_b - \mathbf{N}_b \mathbf{Z}\mathbf{N}_b$  and  $\Delta \mathbf{N} \approx -\mathbf{N}_b \mathbf{Z}\mathbf{N}_b$ .

As an aside, note that had we begun with a compliance formulation, writing strain as an elastic compliance matrix times stress, i.e.  $\varepsilon_j = s_{jk} \sigma_k$ , the strain-stress relations could be written analogously with (3) as

$$\begin{aligned} \mathbf{E}_1 &= \mathbf{A}_i \mathbf{S}_{1i} + \mathbf{C}_i \mathbf{S}_2, \\ \mathbf{E}_{2i} &= \mathbf{C}_i^T \mathbf{S}_{1i} + \mathbf{B}_i \mathbf{S}_2, \end{aligned} \quad (18)$$

then the matrices of the changes from the background compliances due to the presence of the fractures are  $\Delta \mathbf{A} = 0$ ,  $\Delta \mathbf{C} = 0$  and  $\Delta \mathbf{B} = \mathbf{Z}$ .

From the associativity of the process of combining layers, even when there are many types of parallel fractures in the medium, it is the overall compliance of all of them that can be combined to form an 'effective fracture behaviour' which is the average of the different types of fractures weighted by the respective fracture density.

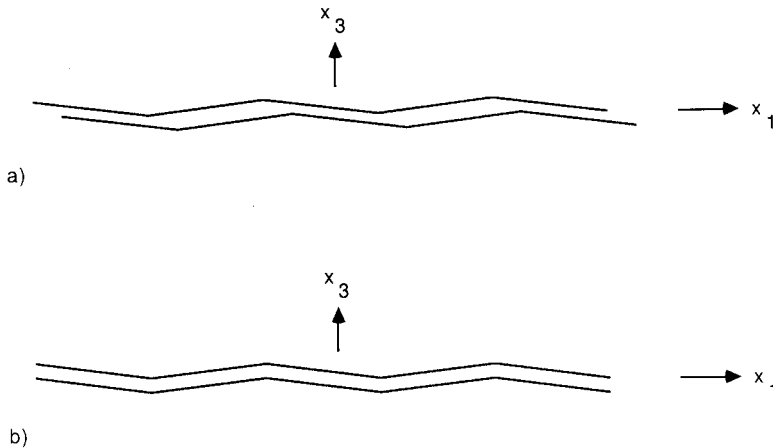


FIG. 1. A schematic of a fracture (a) with monoclinic behaviour and (b) with orthorhombic behaviour. In both cases the ridges cause the tangential traction and tangential slip not to be parallel unless they are either parallel or perpendicular to the ridge axis. In (a), additionally, closure or opening of the fracture will cause tangential slip in the  $x_1$ -direction and vice versa but is uncoupled from tangential motion in the  $x_2$ -direction.

In general, from (15), all three components of the fracture system slip-strain are coupled to all three components of the traction across the fractures. This is the case of triclinic fracture system anisotropy. For this most general behaviour, six parameters are needed to fully describe fracture behaviour within an otherwise homogeneous medium, the six independent components of the fracture compliance matrix  $\mathbf{Z}$ . However, there are three symmetry classes that apply to fracture systems that reduce the number of independent fracture system parameters.

*The monoclinic fracture system.* Let the fracture system be invariant under reflection about a plane containing the  $x_3$ -axis, say the  $x_1$ - $x_3$  plane, implying that  $\mathbf{Z}$  has the form

$$\mathbf{Z} = \begin{bmatrix} Z_N & 0 & Z_{N1} \\ 0 & Z_2 & 0 \\ Z_{N1} & 0 & Z_1 \end{bmatrix}. \quad (19)$$

This shows that fracture slip in the  $x_2$ -direction is uncoupled from normal slip and tangential slip in the  $x_1$ -direction. The  $x_1$ -tangential slip is not uncoupled from normal slip. Tangential fracture displacement and the tangential component of the stress traction are not colinear. Such fracture system behaviour need not be due to the anisotropy of the infilling material, but could be due to slight micro-corrugation of the fracture surfaces, which then must have its peaks and troughs slightly offset, top to bottom, to couple normal and tangential components. This is shown by the schematic diagram in Fig. 1a.

*The orthorhombic fracture system.* Let the fracture system be invariant under reflection about the  $x_1$ - $x_2$  plane uncoupling the fracture system displacement normal to the fractures from the tangential fracture system displacement. Then  $\mathbf{Z}$  has the form

$$\mathbf{Z} = \begin{bmatrix} Z_N & 0 & 0 \\ 0 & Z_2 & Z_{12} \\ 0 & Z_{12} & Z_1 \end{bmatrix}, \quad (20)$$

but there is always a rotation about the  $x_3$ -axis which diagonalizes  $\mathbf{Z}$  giving

$$\mathbf{Z}' = \begin{bmatrix} Z_N & 0 & 0 \\ 0 & Z'_2 & 0 \\ 0 & 0 & Z'_1 \end{bmatrix}. \quad (21)$$

Here,  $Z'_1$  and  $Z'_2$  are the tangential compliances in the  $x'_1$ - and  $x'_2$ -directions respectively. The tangential fracture displacement and the tangential component of the stress traction are not colinear but the normal compliance is uncoupled from the tangential compliance. This can be visualized as a micro-corrugated interface with peaks and troughs aligned, top to bottom (see Fig. 1b). Tangential slip compliance along the corrugation is larger than the tangential slip compliance against the corrugation.

*The transversely isotropic fracture system.* This most symmetrical case occurs when the fracture system behaviour is invariant with respect to rotation about the  $x_3$ -axis. In this case  $\mathbf{Z}$  must have the form

$$\mathbf{Z} = \begin{bmatrix} Z_N & 0 & 0 \\ 0 & Z_T & 0 \\ 0 & 0 & Z_T \end{bmatrix}. \quad (22)$$

$Z_N$  and  $Z_T$  are normal and tangential compliances respectively of an average fracture of dimension length/stress. The tangential fracture displacement and the tangential component of the stress traction are colinear and the normal and tangential compliances are uncoupled. The form of  $\mathbf{Z}$  given here is independent of whether the fracture medium is isotropic or transversely isotropic. However, if the fracture medium were isotropic, stability requires that  $Z_T \geq 4Z_N/3 \geq 0$ . However, if the fracture medium is merely transversely isotropic the stability requires only that  $Z_T$  and  $Z_N$  be non-negative.

The long wavelength equivalent medium to the fractured medium is transversely isotropic only if the fracture system is transversely isotropic, i.e. with  $\mathbf{Z}$  given by (22), and it is embedded in a transversely isotropic background medium which has its symmetry axis perpendicular to the fractures. Then, from (16), and (9)

$$\begin{aligned}
 \mathbf{N}_e &= \begin{bmatrix} c_{33} & 0 & 0 \\ 0 & c_{44} & 0 \\ 0 & 0 & c_{44} \end{bmatrix} = \begin{bmatrix} c_{33b}/(1 + E_N) & 0 & 0 \\ 0 & c_{44b}/(1 + E_T) & 0 \\ 0 & 0 & c_{44b}/(1 + E_T) \end{bmatrix}, \\
 \mathbf{P}_e &= \begin{bmatrix} c_{13} & 0 & 0 \\ c_{13} & 0 & 0 \\ 0 & 0 & 0 \end{bmatrix} = \begin{bmatrix} c_{13b}/(1 + E_N) & 0 & 0 \\ c_{13b}/(1 + E_N) & 0 & 0 \\ 0 & 0 & 0 \end{bmatrix}, \\
 \mathbf{M}_e &= \begin{bmatrix} c_{11} & c_{11} - 2c_{66} & 0 \\ c_{11} - 2c_{66} & c_{11} & 0 \\ 0 & 0 & c_{66} \end{bmatrix} = \begin{bmatrix} c_{11} & c_{11} - 2c_{66b} & 0 \\ c_{11} - 2c_{66b} & c_{11} & 0 \\ 0 & 0 & c_{66b} \end{bmatrix}, \\
 c_{11} &= c_{11b} - \frac{c_{13b}^2}{c_{33b}} \left[ 1 - \frac{1}{1 + E_N} \right],
 \end{aligned} \tag{23}$$

where

$$E_N \equiv c_{33b} Z_N, \quad E_T \equiv c_{44b} Z_T.$$

$E_N$  and  $E_T$  are dimensionless compliances that give the fracture system compliances relative to the background medium compliances, normal and tangential to the fracture system respectively. The modulus matrix depends on seven parameters, the five of the background plus the normal and tangential fracture system compliances. When the background medium is isotropic, the resulting medium is still transversely isotropic, but now depends on four parameters,  $\mu_b$ ,  $\lambda_b$ ,  $E_N$  and  $E_T$ . The moduli are given by (23) with  $c_{11b} = c_{33b} = \lambda_b + 2\mu_b$ ,  $c_{13b} = \lambda_b$  and  $c_{44b} = c_{66b} = \mu_b$ . The matrices of the changes from the isotropic moduli due to the presence of the fractures are

$$\begin{aligned}
 \Delta \mathbf{N} &= - \begin{bmatrix} (\lambda_b + 2\mu_b)E_N/(1 + E_N) & 0 & 0 \\ 0 & \mu_b E_T/(1 + E_T) & 0 \\ 0 & 0 & \mu_b E_T/(1 + E_T) \end{bmatrix}, \\
 \Delta \mathbf{P} &= - \lambda_b \frac{E_N}{1 + E_N} \begin{bmatrix} 1 & 0 & 0 \\ 1 & 0 & 0 \\ 0 & 0 & 0 \end{bmatrix}, \\
 \Delta \mathbf{M} &= - \frac{\lambda_b^2}{\lambda_b + 2\mu_b} \frac{E_N}{1 + E_N} \begin{bmatrix} 1 & 1 & 0 \\ 1 & 1 & 0 \\ 0 & 0 & 0 \end{bmatrix}.
 \end{aligned} \tag{24}$$

This is the very simple model for the behaviour of large joints in an isotropic background. These results agree with those of Morland (1974) and have been used to describe reflectivity from a jointed half-space by Schoenberg (1983).

An isotropic background medium with a transversely isotropic fracture system, as described in (24), is a restricted class of transversely isotropic media. To examine the behaviour of such media, let  $v_{qp}$  be the phase speed of the quasi-compressional wave (the fast wave which is purely longitudinal for propagation parallel and perpendicular to the fractures),  $v_{qs}$  be the phase speed of the quasi-shear wave (the in-plane wave which is purely transverse for propagation parallel and perpendicular to the fractures) and  $v_s$  be the phase speed of the pure shear wave that is always polarized parallel to the fractures. The dimensionless compliances are directly related to the differences between parallel ( $\parallel$ ) and perpendicular ( $\perp$ ) propagation of the squares of the phase speeds normalized by the isotropic background speeds as, from (24),

$$\frac{[v_{s\parallel}^2 - v_{s\perp}^2]}{\mu_b/\rho_b} = \frac{c_{66} - c_{44}}{\mu_b} = \frac{E_T}{1 + E_T} \approx E_T \quad \text{for} \quad E_T \ll 1, \quad (25)$$

$$\frac{[v_{p\parallel}^2 - v_{p\perp}^2]}{(\lambda_b + 2\mu_b)/\rho_b} = \frac{c_{11} - c_{33}}{\lambda_b + 2\mu_b} = 4\gamma_b(1 - \gamma_b) \frac{E_N}{1 + E_N} \approx 4\gamma_b(1 - \gamma_b)E_N \quad \text{for} \quad E_N \ll 1,$$

where  $\gamma_b$  is the square of the ratio of the background shear speed to compressional speed, i.e.  $\gamma_b = \mu_b/(\lambda_b + 2\mu_b)$ . Further, substitution of the perturbations to the elastic moduli from (24) for small  $E_T$  and  $E_N$  (neglecting  $O(E^2)$  terms) into the Christoffel equations for the phase velocity (e.g. see Musgrave 1970) gives

$$\begin{aligned} v_s^2(\theta) &\approx \frac{\mu_b}{\rho_b} [1 - \cos^2 \theta E_T], \\ v_{qs}^2(\theta) &\approx \frac{\mu_b}{\rho_b} [1 - \cos^2 2\theta E_T - \gamma_b \sin^2 2\theta E_N], \\ v_{qp}^2(\theta) &\approx \frac{\lambda_b + 2\mu_b}{\rho_b} [1 - \gamma_b \sin^2 2\theta E_T - (1 - 2\gamma_b \sin^2 \theta)^2 E_N], \end{aligned} \quad (26)$$

where  $\theta$  is the angle between the wavenumber vector and the  $x_3$ -axis. It is clear from (26) that all the phase speeds at all angles are non-increasing with increasing  $E_T$  or  $E_N$ . Note that terms depending on  $\sin^2 2\theta$  or  $\cos^2 2\theta$  are actually  $\cos 4\theta$  terms which have period  $\pi/2$  and are symmetrical about  $\theta = \pi/4$ . Thus for small tangential and normal compliances,  $v_{qs}$  is  $4\theta$ -dependent and is symmetrical about  $\theta = \pi/4$  whereas for  $v_{qp}$ , the tangential compliance yields a  $4\theta$  term symmetrical about  $\theta = \pi/4$  while the normal compliance yields a  $2\theta$  term necessarily not symmetrical about  $\theta = \pi/4$ . Note that tangential compliance by itself, even when it is large, yields only  $4\theta$ -dependence to both  $v_{qp}$  and  $v_{qs}$  (Schoenberg 1983). Tangential compliance contributes a maximum speed decrease for  $v_{qs}$  at  $\theta = 0$  and  $\pi/2$  and no decrease at  $\theta = \pi/4$ . For  $v_{qp}$ , tangential compliance gives maximum decrease at  $\theta = \pi/4$  and no decrease at  $\theta = 0$  and  $\pi/2$ . Normal compliance decreases  $v_{qs}$  in exactly the same way as tangential compliance decreases  $v_{qp}$  while normal compliance decreases  $v_{qp}$  with

maximum decrease at  $\theta = 0$  and minimum decrease at  $\theta = \pi/2$ . The pure shear wave is uncoupled (in the Christoffel equations) from the other two waves. Its greatest speed decrease is at  $\theta = 0$  and there is no decrease at  $\theta = \pi/2$ .

This is a simplified picture due to the assumptions of (1) small fracture compliance relative to the compliance of the unfractured medium, (2) isotropy for the unfractured medium, and (3) transverse isotropy for the behaviour of the fracture system. None the less, (26) indicates the qualitative effects of the presence of large aligned fractures (and, as will be seen below, also of the presence of aligned microcracks) on wave speeds in much more general circumstances.

Equations (24), and the resulting (26), can be compared with the formulation of Thomsen (1986). His three dimensionless anisotropy parameters for weak transverse isotropy,  $\gamma_{Th}$ ,  $\varepsilon_{Th}$  and  $\delta_{Th}$  (the subscript *Th* refers to Thomsen's parameters) along with the shear and compressional wave speed along the symmetry axis of the medium are derivable from the elastic moduli. The three dimensionless parameters express, in general, the deviation of the weakly transverse isotropy from full isotropy. For a fractured medium, the three parameters can be expressed in terms of  $E_T$  and  $E_N$  as

$$\gamma_{Th} = E_T/2, \quad \varepsilon_{Th} = 2\gamma_b(1 - \gamma_b)E_N, \quad \delta_{Th} = 2\gamma_b(E_N - E_T). \quad (27)$$

Thus, the three are not independent for a fractured medium and, until the assumption of microcrack flatness is relaxed, the anisotropy depends only on two parameters,  $E_T$  and  $E_N$ .

### III. JOINTS AND MICROCRACKS

The anisotropy described by the changes of the moduli from an isotropic background, (24), defines a restricted class of transversely isotropic media. Hudson (1981) pointed out that "although the geometry of joints is rather different from that of circular cracks ... under certain conditions, the results are very similar." To see this, we shall examine results from Hudson (1981) and Thomsen (1988) to show that under simple conditions of dilute concentration of very flat microcracks (those where one of the ellipsoidal semiaxes is much less than the other two) in an isotropic background, we can always find joint compliances that give identical values for all the anisotropic elastic moduli. This implies that a seismic experiment giving estimates of the moduli for a Crampin model (azimuthal anisotropy due to the presence of a vertical system of aligned microcracks in an isotropic background which cause the medium to be transversely isotropic with a horizontal axis of symmetry) does not distinguish very well between various types of crack systems. Refinements in the theory of scattering due to flat microcracks will not help in inverting for the crack system's characteristic properties, such as crack size, crack density or the contents of the cracks. Only properties that systems of cracks have in common with those of systems of large vertical joints (such as orientation, excess compliance, relative tangential to normal compliance) have a chance of being determined, but in many instances these could be very informative.

Hudson (1981) gives the general form of the  $6 \times 6$  change of moduli matrix for an isotropic background medium permeated with aligned flat ellipsoidal microcracks to lowest order in wavenumber times mean crack radius  $a$ . For ease of comparison we can express Hudson's matrix (denoted by subscript  $H$ ) using our formulation of three  $3 \times 3$  matrices, giving

$$\begin{aligned} \Delta \mathbf{N}_H &= -e \begin{bmatrix} (\lambda_b + 2\mu_b)(\bar{U}_{33}/\gamma_b) & 0 & 0 \\ 0 & \mu_b \bar{U}_{11} & 0 \\ 0 & 0 & \mu_b \bar{U}_{11} \end{bmatrix} + O(e^2), \\ \Delta \mathbf{P}_H &= -e \lambda_b (\bar{U}_{33}/\gamma_b) \begin{bmatrix} 1 & 0 & 0 \\ 1 & 0 & 0 \\ 0 & 0 & 0 \end{bmatrix} + O(e^2), \\ \Delta \mathbf{M}_H &= -e \frac{\lambda_b^2}{\lambda_b + 2\mu_b} (\bar{U}_{33}/\gamma_b) \begin{bmatrix} 1 & 1 & 0 \\ 1 & 1 & 0 \\ 0 & 0 & 0 \end{bmatrix} + O(e^2). \end{aligned} \quad (28)$$

where  $e$  is the crack density which is equal to the crack number density (number of cracks per unit volume) times  $a^3$ . Note that crack porosity, which is crack number density times the mean crack volume is given by  $\phi_c = 4\pi e a^3 / 3$  where  $\alpha$  is the (very small) mean aspect ratio of the flat ellipsoidal inclusions. The terms  $\bar{U}_{11}$  and  $\bar{U}_{33}$  appearing in (28) arise in the derivation of the scattered field from a single small crack. Essentially  $\bar{U}_{ij}$  is the integral over the face of the crack of the  $i$ th component of the displacement discontinuity due to unit stress  $\sigma_{3j}$  imposed infinitely far from the crack in the  $\pm x_3$ -directions.

Comparing (24) and (28) shows that both flat microcracks and large joints in the same isotropic background give exactly the same moduli if, assuming a dilute concentration of inclusions, we let

$$e \bar{U}_{11} = \frac{E_T}{1 + E_T} \approx E_T \quad \text{for } E_T \ll 1, \quad e \frac{\bar{U}_{33}}{\gamma_b} = \frac{E_N}{1 + E_N} \approx E_N \quad \text{for } E_N \ll 1. \quad (29)$$

Thomsen (1988) points out that the derivations for dilute concentrations of flat aligned microcracks are valid for  $e$  only as large as about 0.05. However, even if second-order terms in  $e$  are included (Crampin 1984), the slip-joint model still conforms to the microcrack model except that there are additional terms proportional to  $e^2$  on the left-hand sides of (29).

Hudson (1981) gives results for  $\bar{U}_{11}$  and  $\bar{U}_{33}$  for three examples which we will write in terms of  $E_T$  and  $E_N$ . Example 1 is for fluid-filled cracks under the assumptions that (a) the tangential component of the traction on the internal crack surfaces is zero (no shear stress) and (b) the crack is so thin that the normal displacement discontinuity across the crack is zero (only tangential displacement discontinuity

across the crack). Then

$$E_T = \frac{16}{3[3 - 2\gamma_b]} e, \quad E_N = 0. \quad (30)$$

Example 2 is for dry cracks under the assumption of zero traction (both normal and tangential) on the internal crack surfaces. These cracks are assumed thick enough to allow non-zero normal displacement discontinuity across the crack.  $E_T$  remains the same but  $E_N$  is non-zero:

$$E_T = \frac{16}{3[3 - 2\gamma_b]} e, \quad E_N = \frac{4}{3\gamma_b[1 - \gamma_b]} e. \quad (31)$$

Example 3 is for cracks filled with a weak solid with small bulk and shear moduli again allowing non-zero normal displacement discontinuity across the crack. Now

$$E_T = \frac{16}{3[3 - 2\gamma_b + 4\mu' / (\pi\alpha\mu_b)]} e,$$

$$E_N = \frac{4}{3\gamma_b[1 - \gamma_b + (\kappa' + (4/3)\mu') / (\pi\alpha\mu_b)]} e, \quad (32)$$

where  $\mu'$  and  $\kappa'$  are the shear and bulk moduli of the inclusion medium respectively. Here terms of order  $\alpha$ ,  $\alpha^2\mu_b/\mu'$  and  $\alpha^2\mu_b/\kappa'$  have been neglected relative to  $\alpha\mu_b/\mu'$  and  $\alpha\mu_b/\kappa'$  (Hudson 1981). Note that for the moduli of the weak solid to affect the values of  $E_T$  and  $E_N$  in (32), the values of  $\mu'$  and  $\kappa'$  must go to zero as the value of the aspect ratio  $\alpha$  goes to zero. This is analogous to the requirement for large joints that the moduli of the infilling material in the joints be proportional to  $h_f$  as  $h_f$  tends to zero. As  $\mu'$  and  $\kappa'$  actually go to 0, the compliances of (32) go to those of (31) for dry cracks.

For  $\kappa'/\mu_b$  and  $\mu'/\mu_b$  not small (of order larger than that of  $\alpha$  as  $\alpha \rightarrow 0$ ),  $E_N$  and  $E_T \rightarrow 0$ . For  $\kappa'/\mu_b$  not small but  $\mu'/\mu_b \rightarrow 0$  as for fluid-filled cracks, (32) go to (30). However, letting  $\kappa'/\mu_b$  be small, of order  $\alpha$  but with  $\mu' = 0$ , approximating cracks filled with weak fluid, gives

$$E_T = \frac{16}{3[3 - 2\gamma_b]} e,$$

$$E_N = \frac{4}{3\gamma_b[1 - \gamma_b + \kappa' / (\pi\alpha\mu_b)]} e$$

$$= \frac{4}{3\gamma_b(1 - \gamma_b)[1 + (3 - 4\gamma_b)\kappa' / 3\gamma_b(1 - \gamma_b)\pi\alpha\kappa_b]} e, \quad (33)$$

where  $\kappa_b = (3 - 4\gamma_b)\mu_b/3\gamma_b$  is the background bulk modulus. Substituting (33) into (26) and (27) gives (3) of Thomsen (1988) for his three anisotropy parameters and resulting phase speeds.

Thomsen (1988) then presented modified results [his (4)] based on the work of Hoenig (1979). These results are similar to (33);  $E_T$  is unchanged but  $\kappa'/\kappa_b$  is replaced by  $(\kappa'/\kappa_b)/[1 - (\kappa'/\kappa_b)]$  in  $E_N$ . When  $\kappa'/\kappa_b \alpha$  is  $O(1)$ ,  $\kappa'/\kappa_b \ll 1$ , there is no

difference between the two sets of results. In the stiff fluid limit, when  $\kappa'/\kappa_b$  (and hence  $\kappa'/\mu_b$  also) is  $O(1)$ ,  $E_N$  is  $O(\alpha)$  and hence tends to zero in both (32) and (33). Thus there is no significant difference between the two sets of results.

Further results are derived by Thomsen (1988) for when the background uncracked medium has equant (non-directional) porosity  $\phi_p$ , i.e. porosity in which the pore space has no dimension significantly larger or smaller than any other and so the pore space can be modelled by spherical pores. His results, again in terms of the dimensionless compliances,  $E_T$  and  $E_N$ , are that  $E_T$  is unchanged due to the presence of equant porosity but  $E_N$ , from  $\varepsilon_{Th}$  [derived by substituting (A34b) into (A16a) Thomsen (1988)] becomes

$$E_N = \frac{4}{3\gamma_b(1-\gamma_b)} \frac{1 - \frac{\kappa'}{\kappa_b(1 + \phi_c/\phi_p)}}{1 + \frac{\kappa'/\kappa_b}{1 - \kappa'/\kappa_b} \left[ \frac{3}{4\gamma_b} + \frac{3 - 4\gamma_b}{3\pi\alpha\gamma_b(1-\gamma_b)} \frac{1}{1 + \phi_p/\phi_c} \right]} e. \quad (34)$$

As  $\phi_p \rightarrow 0$ ,  $E_N$  of (34) goes to Thomsen's (1988) modified result for  $E_N$  with no equant porosity, that is, (33) with  $\kappa'/\kappa_b$  replaced by  $(\kappa'/\kappa_b)/[1 - (\kappa'/\kappa_b)]$ . This may be seen as even when  $\phi_p/\phi_c$  is  $O(1)$  or less, the second term within the brackets of the denominator of (34) dominates the first term due to the presence of the small  $\alpha$ , the aspect ratio, in the denominator of that second term. When  $\phi_p/\phi_c$  is large (which it is in typical sedimentary rocks), so that multiplication by  $\alpha$  gives a term of order unity, the two bracketed terms are of the same order of magnitude. Then in the weak fluid limit,  $\kappa'/\kappa_b \ll 1$ , the right-hand fraction of (34) tends to unity and  $E_N$  tends to the value given for it in (31). For a stiff fluid when  $\kappa'/\kappa_b \rightarrow 1$ , the presence of the  $1 - \kappa'/\kappa_b$  term implies that  $E_N$  becomes small.

#### IV. NON-FLAT ELLIPSOIDAL INCLUSIONS

For all the models discussed so far, an underlying assumption has been that the cracks are flat, i.e. that they can be modelled by ellipsoids with aspect ratio  $\alpha \ll 1$ . These models have all been shown to be identical in behaviour with the medium with large joints (itself an extreme case of aspect ratio  $\rightarrow 0$ ). Nishizawa (1982) calculated the anisotropy due to small concentrations of aligned rotationally-symmetrical ellipsoidal inclusions of any aspect ratio, even including prolate spheroidal inclusions which have an aspect ratio greater than unity. As this is an iterative method using only small increments in crack density at each step, Nishizawa claimed that the method is valid even for large concentrations of inclusions.

Following Nishizawa (1982), the effects of a given crack density  $e$  of ellipsoids are calculated in an iterative way. First the moduli for an isotropic background medium with a crack density of  $e/n$  is calculated, with  $n$  the total number of iterations. Then the moduli for this new 'anisotropic background medium' with

additional crack density  $e/n$  is calculated giving the moduli for the original medium with crack density  $2e/n$ . This is repeated another  $n - 2$  times eventually giving the moduli for the original medium with crack density  $e$ , the desired result. Results can be checked by repeating the calculation with larger values of  $n$  until no change due to increasing  $n$  occurs. The resulting medium is transversely isotropic and we denote the changes in the elastic moduli due to Nishizawa's procedure by  $\Delta c_{ij}^N \equiv c_{ij}^N - c_{ijb}$ . To see how well these moduli, and thus the Nishizawa model, can be approximated by the model of large joints in an isotropic background, we construct  $D^2$ , defined to be one-fifth of the sum of the squares of the differences between the dimensionless moduli changes (over the five independent elastic moduli) from the Nishizawa procedure,  $\Delta c_{ij}^N/c_{ijb}$ ,  $ij = 11, 33, 13, 44, 66$  and the dimensionless moduli changes from the joint model,  $\Delta c_{ij}^J/c_{ijb}$ ,  $ij = 11, 33, 13, 44, 66$ , from (24). The root mean square of the differences of the five elastic moduli  $D$  satisfies

$$5D^2 = \left[ \frac{\Delta c_{11}^N}{\lambda_b + 2\mu_b} + \frac{\lambda_b^2}{(\lambda_b + 2\mu_b)^2} \frac{E_N}{1 + E_N} \right]^2 + \left[ \frac{\Delta c_{33}^N}{\lambda_b + 2\mu_b} + \frac{E_N}{1 + E_N} \right]^2 + \left[ \frac{\Delta c_{13}^N}{\lambda_b} + \frac{E_N}{1 + E_N} \right]^2 + \left[ \frac{\Delta c_{44}^N}{\mu_b} + \frac{E_T}{1 + E_T} \right]^2 + \left[ \frac{\Delta c_{66}^N}{\mu_b} \right]^2. \quad (35)$$

The values of  $E_T$  and  $E_N$  that minimize  $D^2$ , in terms of the Nishizawa moduli  $c_{ij}^N = c_{ijb} + \Delta c_{ij}^N$ , are given by

$$E_T = \frac{\mu_b}{c_{44}^N} - 1, \quad E_N = \frac{\lambda_b^4/(\lambda_b + 2\mu_b)^4 + 2}{\left( \frac{\lambda_b^2/(\lambda_b + 2\mu_b)^2 [c_{11}^N/(\lambda_b + 2\mu_b) - 1 + \lambda_b^2/(\lambda_b + 2\mu_b)^2] + c_{33}^N/(\lambda_b + 2\mu_b) + c_{13}^N/\lambda_b}{\lambda_b + 2\mu_b} \right) - 1}. \quad (36)$$

These values of  $E_T$  and  $E_N$  give the elastic moduli of the joint model that best fit those of the Nishizawa's ellipsoids model in a least-squares sense. Also note that these values of  $E_T$  and  $E_N$  are independent of  $c_{66}^N$  so that the last term of (35) gives a minimum value to  $D^2$  below which no combination of  $E_T$  and  $E_N$  can cause the value of  $D^2$  to fall. However, as the aspect ratio  $\alpha \rightarrow 0$  for any small value of  $e$ ,  $\Delta c_{66}^N$  and  $D$  approach zero. This becomes clear when we calculate the  $c_{ij}^N$  over a wide range of aspect ratio (from  $10^{-3}$  to 1) for gas-filled ellipsoidal inclusions. In a homogeneous isotropic background, with  $\gamma_b = 1/3$  (Poisson's ratio =  $1/4$ ), the gas is assumed to have a vanishing shear modulus and a bulk modulus equal to  $0.0128 \times \mu_b$ . For this model, Fig. 2 shows  $D$  as a function of  $\alpha$  while  $e$  is held constant at three values, 0.001, 0.01 and 0.05.  $D$  is very small for small values of  $\alpha$  and only exceeds 0.05 (which we consider the point where meaningful difference between the joint model and the ellipsoid model begins) for  $e = 0.05$  when  $\alpha > 0.316$  for which crack porosity  $\phi_c > 0.066$ . The same calculations have been carried out for empty

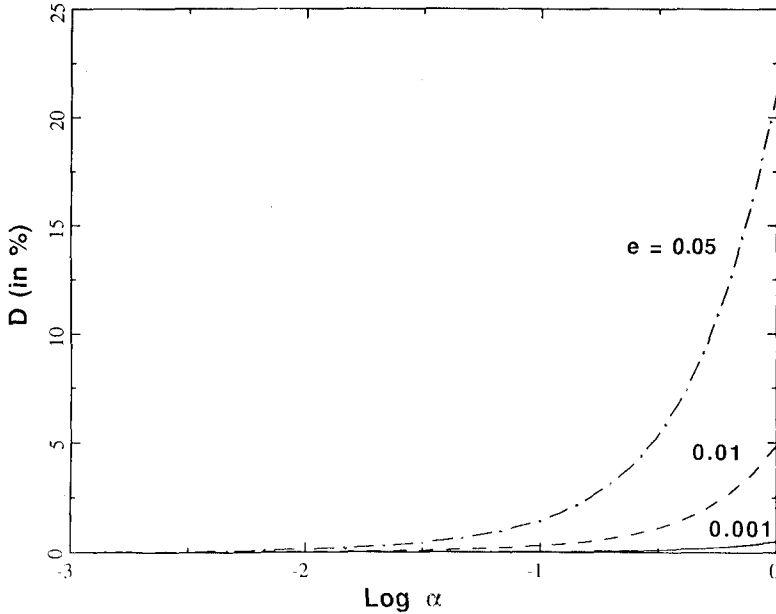


FIG. 2. The root mean square difference  $D$  (in %) between the five elastic moduli computed according to Nishizawa (1982) and those five moduli computed from values of  $E_N$  and  $E_T$  which minimize  $D$  as functions of aspect ratio  $\alpha$  holding  $e$  (the crack number density  $\times$  the mean crack radius cubed) constant. The curve (—) is for  $e = 0.001$ , (---) for  $e = 0.01$  and (-·-·-) for  $e = 0.05$ . The background medium has a Poisson's ratio of  $1/4$  and the ellipsoids are filled with gas assumed to have vanishing shear modulus and a bulk modulus equal to  $0.0128$ —the shear modulus of the background medium.

(dry) inclusions and for liquid-filled inclusions (vanishing shear modulus and bulk modulus equal to  $0.0385 \times \mu_b$ ) giving almost the same results for  $D$ . The values of  $D$  become smaller with the shrinking of the acoustic contrast between the background medium and the material filling the inclusions. The high contrast between the background and the inclusion medium shown here may be thought of as a worst case for matching with the jointed model.

Figure 3 shows  $D$  as a function of  $\alpha$  for the same gas-filled inclusions while crack porosity  $\phi$  (equal to  $4\pi\alpha e/3$ ) is held constant for four values of porosity,  $\phi = 0.01, 0.03, 0.05$  and  $0.07$ . To avoid values of  $e$  larger than  $0.05$ , an approximate upper limit for single scattering theory, each curve starts at the aspect ratio corresponding to  $e = 0.05$ , i.e. at  $\alpha_{\text{start}} = 3\phi/(4\pi \times 0.05)$ . Each curve continues to larger aspect ratios for which the values of  $e$  necessary to maintain constant porosity shrink accordingly.  $D$  increases with increasing aspect ratio whether crack density is held constant or whether porosity is held constant. For these gas-filled inclusions, a porosity of at least  $0.05$  is required for  $D$  to exceed  $5\%$  and that occurs for  $\phi = 0.05$  at aspect ratio  $\alpha = 0.44$  (see Fig. 3).

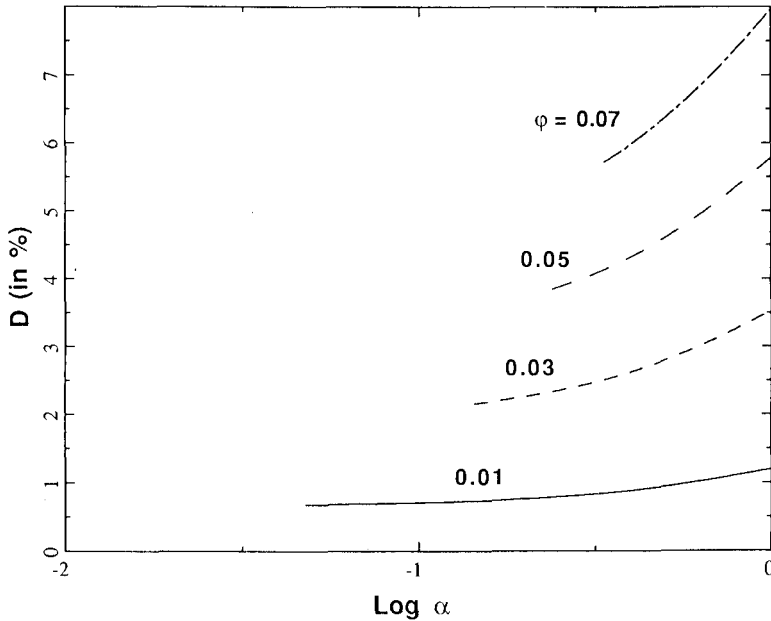


FIG. 3. As for Fig. 2 except here  $D$  is shown as a function of aspect ratio  $\alpha$  holding crack porosity  $\phi$  constant. The curve (—) is for  $\phi = 0.01$ , (-----) for  $\phi = 0.03$ , (-·-·-) for  $\phi = 0.05$  and (-·-·-·-) for  $\phi = 0.07$ .

### DISCUSSION AND CONCLUSIONS

The behaviour of parallel linear-slip interfaces has been used to model the long wavelength propagation characteristics of a medium with a set of large parallel joints or fractures much larger than the largest wavelength but spaced much closer than the smallest wavelength. This model gives geometrical insight into the mechanical properties of such a fractured medium by letting us visualize the action of the planes of weakness in a solid. In addition, we have shown that the linear-slip interface model exactly describes the behaviour of systems of aligned flat microcracks according to Hudson (1981). However, as the aspect ratio of the microcracks grows, i.e. the microcracks become less flat, the results of Nishizawa's (1982) iterative method to compute moduli for a solid with aligned ellipsoidal inclusions deviate increasingly from the linear-slip interface model. But this linear-slip interface model is a good approximation even for aspect ratios as large as 0.3 when  $e = 0.05$  (which is about as large a value of  $e$  as one can assume and still hope that single scattering theory is valid).

All possible types of fracture system anisotropy: triclinic, monoclinic, orthorhombic or transversely isotropic, and all anisotropic elastic backgrounds are included in the model. To compute the elastic moduli of the equivalent medium, once the fracture system compliance matrix is given, requires at most the inversion of two  $3 \times 3$  matrices.

Azimuthal anisotropy has been assumed to be caused by aligned sets of vertical fractures and microcracks. It has been shown that large joints are indistinguishable from dilute systems of flat microcracks. Assuming rotationally isotropic fractures (which is suspect, but perhaps a good first approximation) means that azimuthal anisotropy may be characterized by three scalar quantities, the orientation of the normal to the system and the two compliances,  $Z_T$  and  $Z_N$ . A good approximation to a vertically cracked earth, for which conventional transverse isotropy is often an order of magnitude larger than the azimuthal anisotropy, might be a transversely isotropic (with vertical axis) background with a rotationally isotropic vertical fracture system. Such a model allows for the additional compliance due to the presence of fractures or cracks in a physically meaningful way even when the underlying fracture mechanism is not fully understood. The values of  $Z_T$  and  $Z_N$ , dimensionless with respect to the appropriate background modulus, quantify in the simplest way the azimuthal anisotropy. In many situations it has been shown that the normal compliance can be very small. Assuming that  $Z_N$  vanishes leaves only one parameter quantifying azimuthal anisotropy but this is a key parameter as it still allows for shear-wave splitting for shear waves propagating parallel to the fractures.

#### ACKNOWLEDGEMENT

We thank Schlumberger-Doll Research for their hospitality to one of the authors (J.D.) during the autumn of 1986.

#### REFERENCES

- BACKUS, G.E. 1962. Long-wave anisotropy produced by horizontal layering. *Journal of Geophysical Research* **66**, 4427–4440.
- CRAMPIN, S. 1984. Effective anisotropic elastic constants for wave propagation through cracked solids. *Geophysical Journal of the Royal Astronomical Society* **76**, 135–145.
- CRAMPIN, S. 1985. Evidence for aligned cracks in the Earth's crust. *First Break* **3**, (3), 12–15.
- CRAMPIN, S. and ATKINSON, B.K. 1985. Microcracks in the Earth's crust. *First Break* **3**, (3), 16–20.
- CRAMPIN, S. and BUSH, I. 1986. Shear waves revealed, extensive-dilatancy anisotropy confirmed. 56th S.E.G. meeting, Houston, Expanded Abstracts, 481–484.
- HELBIG, K. and SCHOENBERG, M. 1987. Anomalous polarization of elastic waves in transversely isotropic media. *Journal of the Acoustical Society of America* **81**, 1235–1245.
- HOENIG, A. 1979. Elastic moduli of a non-randomly cracked body. *International Journal of Solids and Structures* **15**, 137–154.
- HUDSON, J.A. 1981. Wave speeds and attenuation of elastic waves in material containing cracks. *Geophysical Journal of the Royal Astronomical Society* **64**, 133–150.
- MORLAND, L.W. 1974. Elastic response of regularly jointed media. *Geophysical Journal of the Royal Astronomical Society* **37**, 435–446.
- MUSGRAVE, M.J.P. 1970. *Crystal Acoustics*, 84–86. Holden-Day, Inc.
- NISHIZAWA, O. 1982. Seismic velocity in a medium containing oriented cracks—transversely isotropic case. *Journal of the Physics of the Earth* **30**, 331–347.

- SCHOENBERG, M. 1980. Elastic wave behavior across linear slip interfaces. *Journal of the Acoustical Society of America* **68**, 1516–1521.
- SCHOENBERG, M. 1983. Reflection of elastic waves from periodically stratified media with interfacial slip. *Geophysical Prospecting* **31**, 265–292.
- SCHOENBERG, M. and MUIR, F. 1988. Group theoretic methods for finely layered media. *Geophysics* (submitted).
- THOMSEN, L. 1986. Weak elastic anisotropy. *Geophysics* **51**, 1954–1966.
- THOMSEN, L. 1988. Elastic anisotropy due to aligned cracks. *Geophysical Journal of the Royal Astronomical Society* (submitted).
- WILLIS, H.A., RETHFORD, G.L. and BIELANSKI, E. 1986. Azimuthal anisotropy, occurrence and effect on shear-wave data quality. 56th S.E.G. meeting, Houston, Expanded Abstracts, 479–481.